

Excluded Volume Effects in Polymer Solutions. 1. Dilute Solution Properties of Linear Chains in Good and Θ Solvents

Ryan C. Hayward and William W. Graessley^{*,†}

Department of Chemical Engineering, Princeton University, Princeton, New Jersey 08544

Received December 11, 1998; Revised Manuscript Received March 15, 1999

ABSTRACT: Data from the literature on four dilute solution properties—radius of gyration, second virial coefficient, intrinsic viscosity, and diffusion coefficient—were analyzed for linear flexible-chain polymers of several species in both thermodynamically good solvents and Θ solvents. Each property was expressed as an effective coil radius, and the ratio of good to Θ solvent radius, the excluded volume expansion factor, was examined over a wide range of chain lengths. The expansion factor, near unity for short chains, crosses over to a power law dependence on chain length for long chains. All data beyond the oligomeric range collapsed to a master curve for each property by a simple rescaling of the chain lengths. The crossovers for these curves are more abrupt than those predicted by the classical theories of polymer solutions. The excluded volume per monomeric unit, obtained by matching experiment and prediction in the power law region, is generally much smaller than the hard sphere prediction in even the best of good solvents. These observations are examined in the light of numerical simulations in the following paper.

Introduction

The dilute solution properties of flexible-chain polymers have been studied for many years. Early investigations were based on viscometric, osmometric, sedimentation, and light scattering intensity measurements. Those techniques were later supplemented by dynamic light scattering and by small-angle neutron and X-ray scattering. Nearly monodisperse samples were used in most studies, supplied at first by fractionation procedures and later by anionic polymerization. The combination of these experiments with theories based on the random-coil model has led to a rather good understanding of the solvent-mediated intramolecular interactions in the dilute regime, excluded volume, and hydrodynamic coupling.^{1–6}

A longtime goal, pursued most recently in a series of investigations by Yamakawa, Einaga, and co-workers, is the detailed description of behavior over the full range of sizes. They employ the helical wormlike chain (HWC) model to describe the properties of chains in the small to intermediate size range.⁷ Their work has had the additional benefit of making available an extensive new body of high-quality data for linear chains of several species, filling out what had been a rather sparse collection of results in the smaller size range. In this paper, we combine the Yamakawa–Einaga data with earlier results in order to investigate the apparent weakness of excluded volume effects in even the best of good solvent systems.⁸ We focus on the behavior of flexible chain species in good solvents only. Data for short chains are included, but the interpretation emphasizes intermediate and long chains, and it omits any detailed consideration of HWC effects. We also do not consider excluded volume effects in the region near the Θ condition or polymer species with large persistence lengths. The effects of excluded volume on various dilute solution properties are expressed, insofar as possible,

in the form of master curves that contain the particularities of species in the reducing parameters alone. Molecular interpretation is deferred until the validity of this approach, a generalized form of the two-parameter theory of dilute polymer solutions,⁷ is established. A similar approach is used in the following paper⁹ to organize the results of Monte Carlo simulations for self-avoiding chains with varying strengths of self-attraction.

Four dilute-solution properties are considered—radius of gyration R_g , second virial coefficient A_2 , intrinsic viscosity $[\eta]$, and diffusion coefficient D_0 . The first two are equilibrium properties, the other two are dynamical. Each property varies with chain length, as represented here by the molecular weight M , and each depends on the solution thermodynamics. To facilitate comparison among effects on the various properties, we have expressed each as a molecular size. The radius of gyration is of course already a size, and the others are converted to effective sizes by means of expressions for hard sphere solutes¹⁰

$$R_t = \left(\frac{3 A_2 M^2}{16\pi N_a} \right)^{1/3} \quad (1)$$

$$R_v = \left(\frac{3 [\eta] M}{10\pi N_a} \right)^{1/3} \quad (2)$$

$$R_h = \frac{k_B T}{6\pi\eta_s D_0} \quad (3)$$

in which R_t , R_v , and R_h are the thermodynamic, viscometric, and hydrodynamic radii, N_a is Avogadro's number, k_B is Boltzmann's constant, T is the temperature, and η_s is the solvent viscosity.

Excluded volume at the binary interaction level is canceled at the Θ condition, so $(R_t)_\Theta = 0$. For long-enough chains the other sizes vary with chain length in the random-walk manner:

[†] Current address: 7496 Old Channel Trail, Montague, MI 49437.

$$(R_g)_\Theta = K_s M^{1/2} \quad (4)$$

$$(R_v)_\Theta = K_v M^{1/2} \quad (5)$$

$$(R_h)_\Theta = K_h M^{1/2} \quad (6)$$

The expansion of molecular size in good solvents caused by volume exclusion is quantified by an expansion factor denoted by α . Thus,

$$\alpha_s = \frac{R_g}{(R_g)_\Theta} \quad (7)$$

$$\alpha_v = \frac{R_v}{(R_v)_\Theta} = \left(\frac{[\eta]}{[\eta]_\Theta} \right)^{1/3} \quad (8)$$

$$\alpha_h = \frac{R_h}{(R_h)_\Theta} \quad (9)$$

For uniformity of discussion we have included the available data for A_2 in the expansion factor formalism but, since $(R_t)_\Theta = 0$, doing that requires a different method for normalizing the good solvent values. Davidson et al.¹⁰ noted that ratios of radii such as R_t/R_v and R_h/R_g have values in the long-chain region that are relatively insensitive to chain length and to the solution thermodynamics as well. We use that observation to construct an R_t normalization size from $(R_g)_\Theta$ and a value for R_t/R_g in good solvents. The values of R_t/R_g are similar for the three good solvent systems discussed in ref 10. The average, 0.676, is used to define the R_t normalization size, $0.676(R_g)_\Theta$, and from that a thermodynamic expansion factor:

$$\alpha_t = \frac{R_t}{0.676(R_g)_\Theta} \quad (10)$$

Data obtained from the literature sources listed in Table 1 are considered for eight polymer species: polystyrene [PS], poly(α -methylstyrene) [P α MS], atactic poly(methyl methacrylate) [aPMMA], isotactic poly(methyl methacrylate) [iPMMA], polyisobutylene [PIB], poly(dimethylsiloxane) [PDMS], 1,4-polybutadiene [PBD], and 1,4-polyisoprene [PI]. (The last two are statistical copolymers of 1,4-cis and 1,4-trans units, and they also contain ~8% 1,2 or 3,4 units. The isomeric proportions vary insignificantly with chain length for the samples studied, so PBD and PI are homopolymers in the context of this study.) All samples are linear and have narrow molecular weight distributions. Their molecular weights were determined by a variety of absolute techniques, although a scattering method giving M_w was most commonly used. Since the distributions are narrow, the type of averaging is relatively unimportant, so we have dropped the subscript and are simply using M to designate the molecular weight.

Some of the references include compilations of earlier data.^{23,37} In particular, ref 23 contains extensive data from the Fujita laboratory^{44–49} and the studies of Burchard and co-workers.^{50,51} We have omitted results published prior to 1965. Our search was not exhaustive, and some good data may have been overlooked, particularly in the case of polystyrene, which has been studied carefully by many groups.

Analysis of Data

Properties in good solvents and at the Θ condition were examined for each species over the widest possible

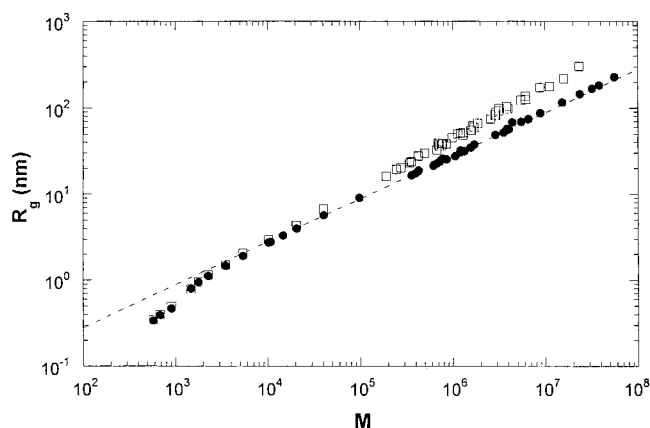


Figure 1. Relationship between radius of gyration and molecular weight for polystyrene in cyclohexane at Θ (●) and in toluene (□). The dashed line indicates the best fit to limiting behavior at Θ , given in Table 2.

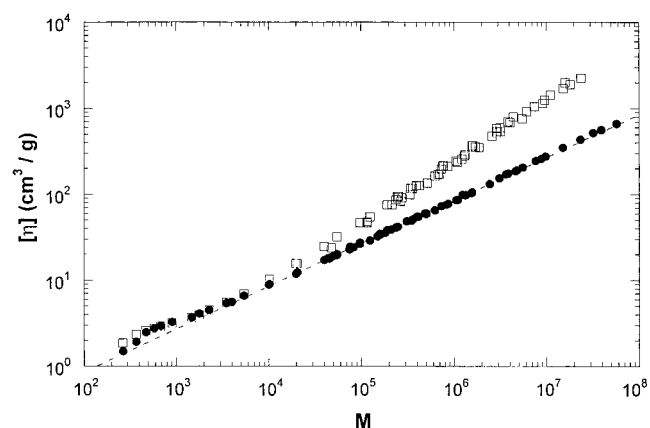


Figure 2. Relationship between intrinsic viscosity and molecular weight for polystyrene in cyclohexane at Θ (●) and in toluene (□). The dotted line indicates the best fit to limiting behavior at Θ , given in Table 2.

range of chain lengths. Preliminary examination of the data indicated significant differences in the coil size for individual samples among the various good solvents, so the behavior in each good solvent system was analyzed separately. Data were available in only one Θ solvent for most species. For PS, however, results in four Θ solvents were available—cyclohexane (for which there is the most data), *trans*-decalin, Decalin (a mixture of cis and trans isomers), and dioctyl phthalate. Results in two Θ solvents, benzene and isoamyl isovalerate, were available for PIB. Also, different researchers using the same Θ solvent for a given species sometimes report slightly different values of the Θ temperature. In nearly all cases, however, close agreement was found between the data from different investigators, even when different values of the Θ temperature, or different Θ solvents, were used. The only exception was PDMS, for which the results in two Θ solvents, methyl ethyl ketone and bromocyclohexane, disagreed significantly. We chose to disregard the methyl ethyl ketone data since the results in bromocyclohexane are more extensive.

Behavior that is typical of all the polymer species is illustrated in Figures 1 and 2, which show R_g and $[\eta]$ as functions of M for PS in cyclohexane (Θ condition) and toluene (good solvent). As illustrated in these figures and well-known for many years, Θ condition values of both R_g and $[\eta]$ are characterized throughout the intermediate- and long-chain region by a linear

Table 1. Sources of Data Used in the Study

solvent	refs			
	R_g	$[\eta]$	D_0	A_2
		PS		
cyclohexane ^a	11, 12, 23	13, 14, 21, 22, 23	17, 23	
decalin		11		
trans-decalin	21	21	19	
dioctyl-phthalate		11		
benzene	20, 21, 23	13, 15, 20, 21, 22, 23	23	20, 21, 23
toluene	11, 12, 18, 20, 23	11, 14, 20, 23	16, 23	11, 18, 20, 23
ethylbenzene	23	23	23	23
dichloroethane	20	20		20
4-tert-butyltoluene	18	16	16	18
n-butyl chloride	18			18
tetrahydrofuran	23	23	23	23
		aPMMA		
acetonitrile	24, 25	25, 27	29	
n-butyl chloride		25, 27		
nitroethane	25	25		31
chloroform	25	25		31
acetone	25	25	29	31
		iPMMA		
acetonitrile	26, 28	30	29, 30	
nitroethane				32
chloroform	28	28		32
acetone	28	28	29	32
		PIB		
isoamyl isovalerate	32, 33, 36	12, 33, 34, 35, 36	34, 36	
benzene		33, 35		
cyclohexane	33, 36	33, 36	36	33, 36
n-heptane ^b	12, 33, 36, 37, 38	12, 33, 34, 36	34, 36	33, 36
		PDMS		
bromocyclohexane	19, 41	39, 41	39	
methylethyl ketone		39, 41		
toluene	40, 41	40, 41	40	41
cyclohexane		41		
		PBD		
1,4-dioxane	23	23	23	
cyclohexane	23	23, 42	23	23, 42
tetrahydrofuran		42		
		PI		
1,4-dioxane	23, 43	23, 43	23	
cyclohexane	23	23	23	23
		P(αMS)		
cyclohexane	23	23	23	
toluene	23	23	23	23

^a Berry¹¹ uses a variety of Θ solvents, including cyclohexane and several mixtures of decalin isomers. ^b Values of R_g at low molecular weights³⁷ were measured in *n*-decane.

Table 2. Coefficients for Dilute Solution Relationships at the Θ Condition

polymer	$(R_g/M^{1/2})_\Theta$ (nm)	$([\eta]/M^{1/2})_\Theta$ (cm ³ /g)	$(R_h/M^{1/2})_\Theta$ (nm)
PS	0.028	0.085	0.022
PαMS	0.028	0.074	0.021
aPMMA	0.025	0.055	0.020
iPMMA	0.030	0.093	0.0235
PDMS	0.0295	0.083	0.022
PIB	0.031	0.11	0.024
PI	0.0333	0.13	0.026
PBD	0.0377	0.18	0.028

dependence on $M^{1/2}$. This was found to be the case for $(R_g)_\Theta$, $(R_h)_\Theta$, and $[\eta]_\Theta$ for all the species. Coefficients relating each of the unperturbed properties to its asymptotic $M^{1/2}$ form are given in Table 2. They were determined by visual fits of the data because the judgment required to locate the onset of asymptotic behavior made it difficult to apply least-squares fitting.

In the short-chain region, values in good solvents and Θ solvents are nearly the same, as exemplified in

Figures 1 and 2, although each may deviate from the $M^{1/2}$ behavior. This deviation reflects a species-dependent breakdown of the random coil model in the short chain region and, for the dynamic properties, of variations in hydrodynamic penetration as well.⁷ Interesting oddities such as negative intrinsic viscosities appear in this range (PIB and PDMS). At somewhat higher molecular weights the Θ solvent data begin to display the aforementioned $M^{1/2}$ dependence, but with good solvent values the same or only slightly larger than the corresponding to Θ solvent values. Finally, beyond a certain molecular weight range, which depends on both the property and the polymer-solvent system, sizes in the good solvents begin to depart significantly from the Θ solvent sizes, with the good solvent sizes eventually taking on their limiting power-law dependence on chain length.

Values of the expansion factor were obtained somewhat differently in the short-chain and long-chain regions. Considerable amounts of data for long chains in good solvents were available on samples for which

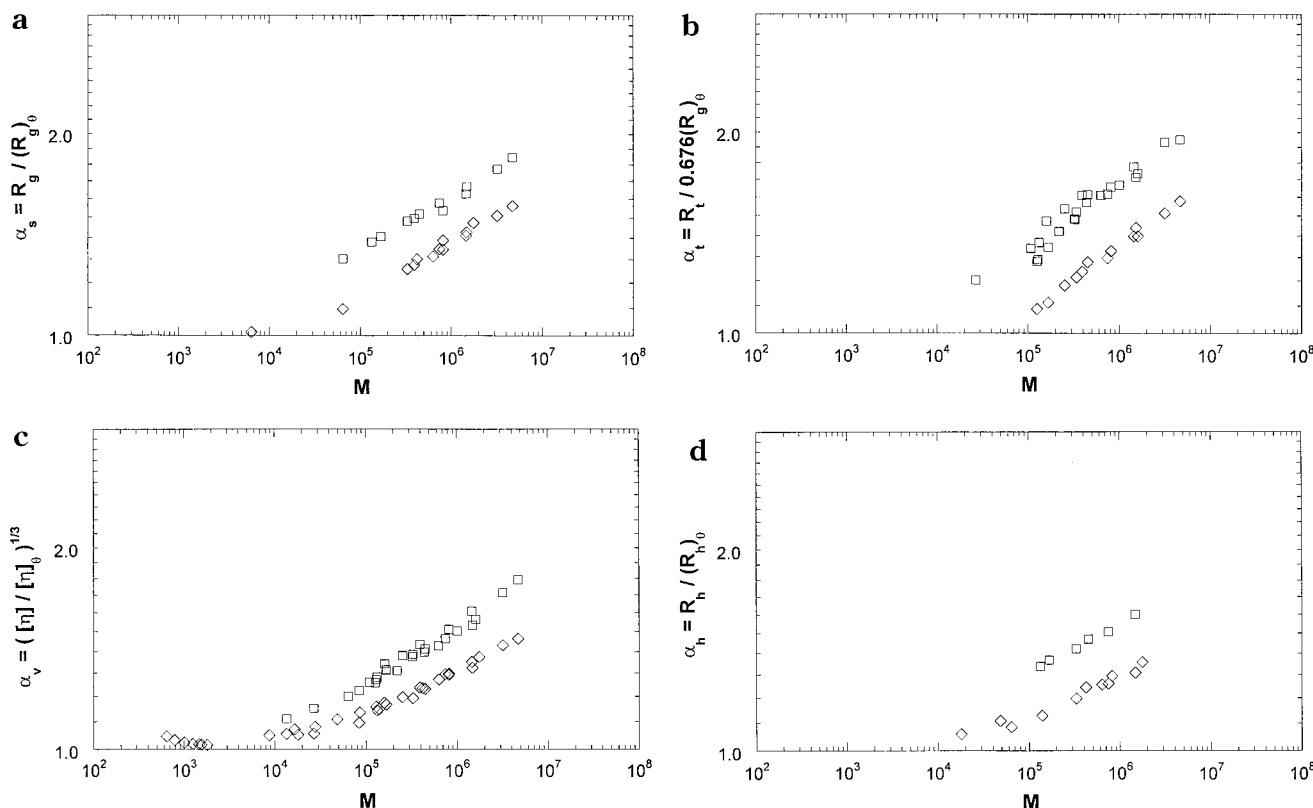


Figure 3. Expansion factor vs molecular weight for polyisobutylene in good solvents *n*-heptane (\diamond) and cyclohexane (\square): (a) α_s ; (b) α_t ; (c) α_v ; (d) α_h .

no corresponding to Θ solvent measurement had been made. To make use of these data and yet treat all results uniformly, expansion factors for the medium- to long-chain region were calculated by the *long-chain method*, i.e., by applying eqs 7–10 to the observed good solvent size and to a Θ solvent size calculated with the molecular weight and the appropriate equation from Table 2. For example, the size expansion factor was calculated as

$$\alpha_s = \frac{R_g}{K_s M^{1/2}} \quad (11)$$

with K_s for each species taken from Table 2.

Equations 4–6 do not accurately describe short-chain behavior in Θ solvents, as Figures 1 and 2 demonstrate. In this region, expansion factors were calculated by the *short-chain method*—by applying eqs 7–9, but using only values measured in both Θ and good solvents for the same sample. The short-chain method was used wherever possible, so, as shown in subsequent figures, there is considerable overlap of results from the two methods. We have no basis for applying eq 10 to short chains, so α_t was not evaluated in this region.

Figure 3 illustrates some characteristics of the expansion factors for long chains with data for PIB in two good solvents, *n*-heptane and cyclohexane. The results are typical of those found in the other polymer–solvent systems. Thus, the relationship between α_x and M ($x = s, t, v, h$) varies from one polymer species to another and, for a given species, from one good solvent to another. However, the forms of each of these relationships are similar: the data for different polymer–solvent systems can be superimposed by a simple rescaling of the molecular weight, i.e., by translation of

Table 3. Limiting Power-Law Exponents for the Expansion Factors

expansion factor	exponent
α_s	0.092 ± 0.003
α_t	0.088 ± 0.002
α_v	0.079 ± 0.001
α_h	0.077 ± 0.006

$\log \alpha_x$ vs $\log M$ plots parallel to the $\log M$ axis. Superposition was the most convincing and produced the least scatter for α_t and α_v . The somewhat larger spread of values encountered with α_s and α_h was due to scatter in the data for the individual polymer–solvent systems and not to poor superposition of otherwise well-defined curves.

For each of the four expansion factors, the results for one polymer–solvent system with well-defined behavior over a wide range of molecular weights was used as a reference, and results for the other systems were shifted to coincide with that reference curve. Once satisfactory superposition had been achieved, as judged visually, a least-squares regression was performed to obtain a power-law fit for the long-chain region. The limiting exponents so obtained for each property— p_s , p_t , p_v , and p_h —are given in Table 3. To remove the dependence of the best-fit equations on an arbitrary reference system, the molecular weights for each polymer–solvent pair were normalized by a scale factor denoted as M^\dagger , which corresponds to the intersection of the limiting power law with $\alpha = 1$. Thus, in the long chain region, the expansion factors for each polymer–solvent system are expressed as

$$\alpha_s = \left(\frac{M}{M^\dagger} \right)^{p_s} \quad (M \gg M^\dagger_x) \quad (12)$$

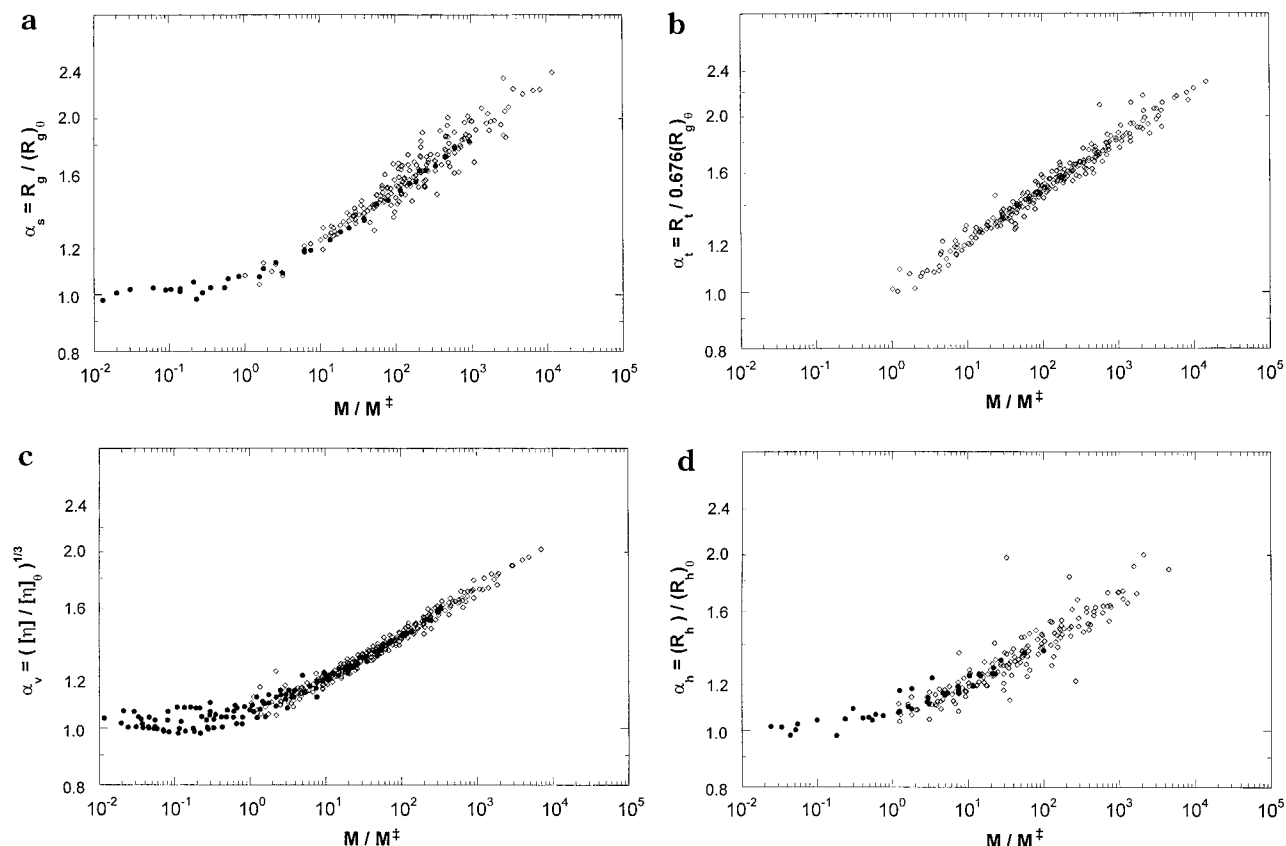


Figure 4. Expansion factors vs reduced molecular weight, evaluated in the short-chain method (●) and the long-chain method (◇): (a) α_s ; (b) α_t ; (c) α_v ; (d) α_h .

Table 4. Characteristic Molecular Weights for Various Polymer–Solvent Systems^a

polymer	solvent	M_s^*	M_t^*	M_v^*	M_h^*	$(M^*)_{av}$
PS	benzene	4800	3880	8070	(14000)	7700
	toluene	(6420)	(4200)	12800	(13200)	9200
	dichloroethane	12000	8090	14800		11600
	ethylbenzene	(8280)	7600	19500	(30300)	16400
PaMS	tetrahydrofuran	(7660)	2590	10800	(4920)	6500
	toluene	(12400)	8090	16800	(19300)	14200
aPMMA	acetone	19900	19700	33000		24200
	nitroethane	4430	3070	6730		4700
	chloroform	950	420	1010		790
	benzene			3700		3700
iPMMA	acetone	50490	129000	87400		89000
	nitroethane		10700			10700
	chloroform	2070	1680	2820		2200
PDMS	toluene	13000		18000	17800	16300
	cyclohexane			7740		7700
PIB	<i>n</i> -heptane	27700	29800	33000	30300	30200
	cyclohexane	5790	2940	5180	3220	4300
PI	cyclohexane	(2690)	3400	3770	3480	3400
PBD	cyclohexane	10300	5500	5720	8700	7600
	tetrahydrofuran			4700		4700

^a Values in parentheses are somewhat less certain than the others.

For each polymer–solvent system, M_x^* is a crossover molecular weight ($x = s, t, v, h$) that specifies the range where significant departures from the Θ -condition size begin. Values of M_x^* obtained for the various properties, species, and good solvents are given in Table 4.

Plots of α_x vs M/M_x^* for both long- and short-chain data are shown in Figure 4. In the overlap region there is good agreement between data analyzed in the short-chain and long-chain methods. The transition near M_x^* is a relatively abrupt one. That is, at molecular weights below M_x^* , the expansion factors quickly approach and then scatter around unity, while not far above M_x^* the

behavior is already well described by the power law. Note, however, that our method of forming the master curves and assigning the values of M_x^* relies almost entirely on the long-chain data. Accordingly, any features reflecting species-dependent behavior in the short-chain region, and hence unlikely to scale with M/M_x^* , would be obscured.

Discussion

Expansion Factor Parameters. The four limiting power-law exponents (Table 3) do not differ greatly from one another. Within the uncertainties, those for the equilibrium properties, p_s and p_h , are indistinguishable. The same is true for the dynamic-property exponents, p_v and p_h . Indeed, whatever differences there might be between the chain-length dependence of R_t and R_g is lost in the data scatter, as shown by the plot of R_t/R_g vs M/M^* in Figure 5. The average for $M > M^*$, $R_t/R_g = 0.668 \pm 0.005$, is essentially the same as reported by Davidson et al.¹⁰ and is in excellent accord with $R_t/R_g = 0.690$ from Monte Carlo simulations of self-avoiding walks.⁵² The chain-length dependence of the dynamic sizes is similarly indistinguishable, as shown by the plot of R_v/R_h in Figure 6. The average for $M > M^*$ is $R_v/R_h = 1.073 \pm 0.005$ in good solvents and 1.064 ± 0.006 at Θ .

Merged plots for α_{eq} (α_s and α_t) and for α_{dyn} (α_v and α_h) are shown as functions of M/M^* in Figures 7 and 8. Limiting exponents for the merged plots are

$$\begin{aligned}
 p_{eq} &= 0.089 \pm 0.001 \\
 p_{dyn} &= 0.078 \pm 0.001
 \end{aligned}
 \quad (13)$$

Within the uncertainties, the value for p_{eq} agrees well with the α_s exponent from renormalization group

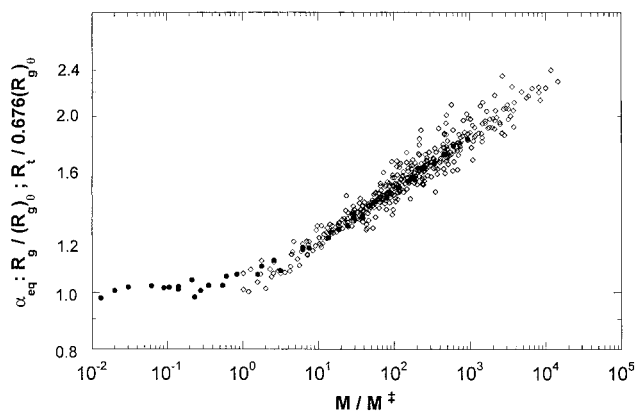


Figure 5. Merged expansion factor for equilibrium properties vs reduced molecular weight, evaluated in the short-chain (●) and long-chain (◇) manner.

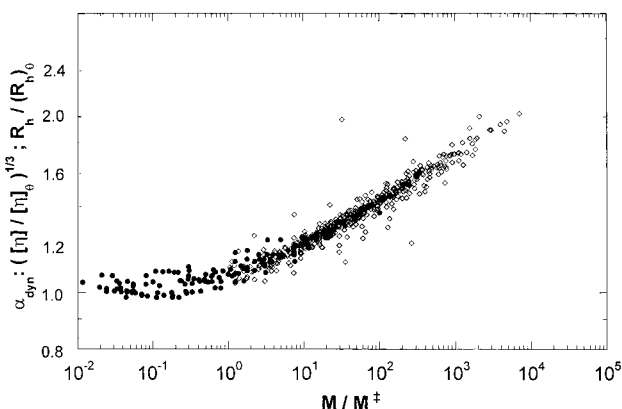


Figure 6. Merged expansion factor for dynamic properties vs reduced molecular weight, evaluated in the short-chain (●) and long-chain (◇) manner.

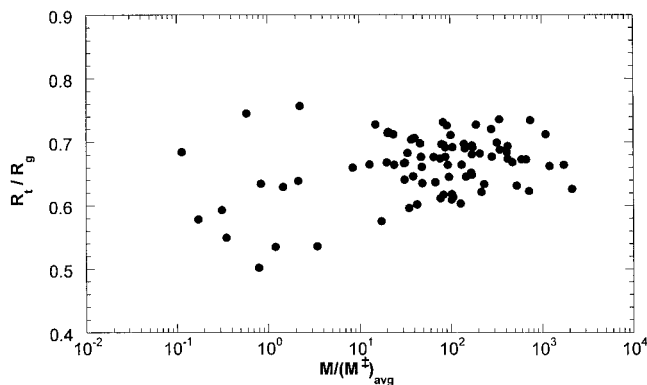


Figure 7. Ratio of equilibrium sizes vs reduced molecular weight for all species in good solvents.

theory,⁵³ $(0.5880 - 1/2) = 0.0880$, and with the exponent for both α_s and α_t from the Monte Carlo simulations,⁵² 0.0877. The exponent for dynamic properties is discernibly smaller than for equilibrium properties. Finally, based on the experimental results in this study, the limiting exponent in good solvents for R_g is $0.5 + p_{eq} = 0.589 \pm 0.001$, and that for $[\eta]$ is $0.5 + 3p_{eq} = 0.734 \pm 0.004$.

The characteristic molecular weights for the onset of coil expansion effects (Table 4) vary somewhat erratically from one property to another. Thus, the various values of M^*_x for a polymer–solvent system sometimes differ by a factor of 2 or more. In most cases M^*_v and M^*_h agree fairly well, and they are larger than M^*_s and M^*_t by an average of about 30%. Otherwise, there seems

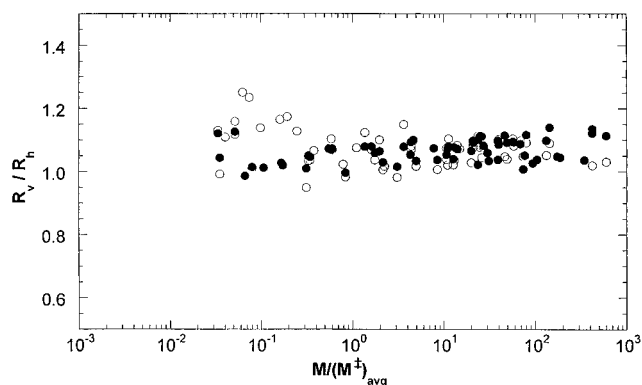


Figure 8. Ratio of dynamic sizes vs reduced molecular weight for all species in Θ solvents (○) and good solvents (●).

to be no particular pattern in the differences. The average of all values for each polymer–solvent system, $(M^*)_{av}$, is listed in Table 4.

Master Curve Forms. The transition of the size expansion factor, from short-chain values near unity to the long-chain power law, is more abrupt than predicted by the commonly used theoretical forms.^{1,7} The crossover is quite a gradual one according to the Flory expression¹

$$\alpha_s^5 - \alpha_s^3 = 1.276z \quad (14)$$

in which z is the excluded volume parameter

$$z = \left(\frac{1}{4\pi}\right)^{3/2} \frac{\beta}{(R_g^3)_\Theta} \left(\frac{M}{m_0}\right)^2 \quad (15)$$

where m_0 is the molecular weight per monomeric unit, M/m_0 is the number of monomeric units per chain, and β is the binary cluster integral for monomeric units. The crossover is less gradual for the Domb–Barrett interpolation formula, which those authors choose to express in terms of the expansion factor for end-to-end distance:⁵⁴

$$\alpha_R = \left[1 + 10z + \left(\frac{70\pi}{9} + \frac{10}{3}\right)z^2 + 8\pi^{3/2}z^3\right]^{1/15} \quad (16)$$

It is still not as abrupt, however, as the observed behavior, as shown below.

Both eqs 14 and 16 lead to the Flory power law exponent in the long-chain limit: with $z \propto M^{1/2}$ from eq 15, each has the limiting form $\alpha_s \propto M^{1/10}$. To facilitate comparisons of crossover behavior for different properties, we force the limiting exponents to agree with the observed values (Table 3), by replacing α_s^5 in eq 14 with $\alpha_s^{5.46}$ and the exponent $1/15$ in eq 16 with $1/16.38$, and express them in terms of M^*_s through eq 12. Thus, the Flory expression becomes

$$\alpha_s^{5.46} - \alpha_s^3 = \left(\frac{M}{M^*_s}\right)^{1/2} \quad (17)$$

in which

$$M^*_s = \frac{M}{(1.276z)^2} \quad (18)$$

An equation analogous to the Domb–Barrett expression (eq 16) was developed for the size expansion factor

$$\alpha_s = \left[1 + 2.945 \left(\frac{M}{M_s^\dagger} \right)^{1/2} + 2.449 \left(\frac{M}{M_s^\dagger} \right) + \left(\frac{M}{M_s^\dagger} \right)^{3/2} \right]^{0.0611} \quad (19)$$

in which

$$M_s^\dagger = \frac{M}{4\pi z^2} \quad (20)$$

The new equation has the observed limiting exponent p_s but still preserves the correct coefficients of z and z^2 in the series expansion for size.¹

Equations 17 and 19 are compared with the size expansion data in Figure 9. The crossover predicted by the modified Flory expression is much too broad, as mentioned above, and the modified Domb–Barrett expression, while lying much closer to the data, is still not entirely satisfactory. The experimental results are fitted rather well by the following further modification of the Flory expression, which is shown as the solid curve in Figure 9:

$$\alpha_s^{5.46} - \alpha_s^{-20} = \left(\frac{M}{M_s^\dagger} \right)^{1/2} \quad (21)$$

Equation 21 is now wholly empirical, having no significance beyond demonstrating that the observed crossover is abrupt enough to require what is essentially an exponential cutoff of the second term beyond $M = M_s^\dagger$. We employ it merely to provide a concise and accurate description of what appears to be universal behavior for good solvents over the full range of sizes beyond the oligomeric range. A slightly different modified form fits the viscometric size ratios:

$$\alpha_v^{6.30} - \alpha_v^{-10} = \left(\frac{M}{M_v^\dagger} \right)^{1/2} \quad (22)$$

Comparison with data and with the modified Flory form (eq 17) is shown in Figure 10.

Interpretation of M_s^\dagger . Values of the binary cluster integral for monomeric units were calculated from M_s^\dagger with eqs 15 and 18:

$$\beta = \left(\frac{(4\pi)^{1/2} R_g}{M^{1/2}} \right)_\Theta^3 \frac{m_o^2}{1.276 (M_s^\dagger)^{1/2}} \quad (23)$$

The same form is obtained by combining eqs 15 and 20, the only difference being replacement of the numerical factor 1.276 by $2\pi^{1/2} = 3.54$. The values calculated for each polymer–solvent system—with $(R_g/M^{1/2})_\Theta$ from Table 2, $(M^\dagger)_{av}$ from Table 4, and the molecular weight of the monomeric unit—are given in Table 5. Values of $(M^\dagger)_{av}$ were used instead of M_s^\dagger because of their greater reliability and availability for all systems; use of M_s^\dagger would increase the values of β by an average of 15%. The hard-sphere value of the binary cluster integral for monomeric units, β_{hs} , was also calculated¹

$$\beta_{hs} = 8v_o = \frac{8m_o \phi}{\rho N_a} \quad (24)$$

in which v_o is the hard-core volume per monomeric unit, ρ is the mass density of the undiluted polymer liquid,⁵⁵ and ϕ is the packing fraction (hard core volume)/(total liquid volume). We used an estimated packing fraction,⁵⁶

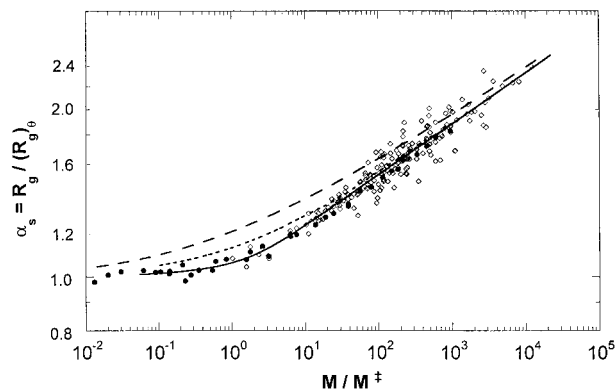


Figure 9. Expansion factor for radius of gyration vs reduced molecular weight evaluated by the short-chain method (●) and the long-chain method (◇). The solid line is eq 21, the expression fitted to the data. The dashed line is eq 17, the Flory expression adjusted to fit the observed limiting dependence of α_s on M . The dotted line is eq 19, the similarly adjusted Domb–Barrett expression.

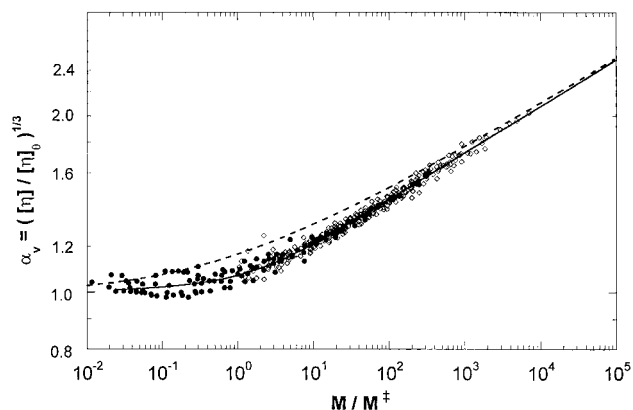


Figure 10. Expansion factor for viscometric size vs reduced molecular weight evaluated by the short-chain method (●) and the long-chain method (◇). The solid line is eq 22, the dashed line eq 17.

Table 5. Excluded Volume Parameters

polymer	solvent	β (nm ³)(a)	β_{hs} (nm ³)(b)	β/β_{hs}
PS	benzene	0.095	0.73	0.13
	toluene	0.087	0.73	0.12
	dichloroethane	0.077	0.73	0.11
	ethylbenzene	0.065	0.73	0.089
	tetrahydrofuran	0.10	0.73	0.14
PαMS	toluene	0.090	0.81	0.11
	acetone	0.035	0.62	0.056
	nitroethane	0.080	0.62	0.13
	chloroform	0.19	0.62	0.31
iPMMA	benzene	0.090	0.62	0.145
	acetone	0.032	0.62	0.052
	nitroethane	0.091	0.62	0.147
	chloroform	0.20	0.62	0.32
PDMS	toluene	0.039	0.57	0.068
	cyclohexane	0.056	0.57	0.10
PIB	n-heptane	0.020	0.46	0.043
	cyclohexane	0.054	0.46	0.12
PI	cyclohexane	0.055	0.50	0.11
PBD	cyclohexane	0.063	0.44	0.14
	tetrahydrofuran	0.080	0.44	0.18

$\phi = 0.55$, for all species. The values of β_{hs} so obtained are listed in Table 5.

The values of β in Table 5 are seen to be considerably smaller than the hard sphere value β_{hs} . The ratio β/β_{hs} , shown in the last column of Table 5, is about 0.1 or smaller in all systems except iPMMA and aPMMA in chloroform. Even in the best of good solvents, the chain

units apparently experience a mutual attraction that is enough to offset nearly the entire hard-core repulsion. The discrepancy seems too large to be dismissed as an artifact of crudeness from the representation of polymer chains as dilute arrays of mutually excluding spheres. This is the crux of the Fujita concern about the apparently general weakness of excluded volume effects.⁸

On the other hand, representing the chain as a dilute array of unconnected spheres, the basis of eq 23, is certainly crude in the extreme. Strings of spheres would no doubt be preferable to unconnected arrays for modeling self-avoiding chains in dilute solution, and strings of rods with appropriately chosen diameters and lengths might be even better. It is thus conceivable that the equivalent hard-core volume, β_{hc} , would be significantly reduced if more realistic models of flexible chains were used,^{59,60} making β/β_{hc} much nearer unity. None of these physically more reasonable models has in fact been applied to the problem, however, so the discrepancy remains in principle unresolved. The numerical simulation study described in the following paper⁹ was undertaken in the hope of settling this quandary.

Acknowledgment. We are grateful to Guy Berry, Walther Burchard, Hiroshi Fujita, and Jacques Roovers for their very helpful criticisms of an earlier version of the paper. We also gratefully acknowledge the financial support of this work provided by the National Science Foundation through a grant to Princeton University (DMR-9310762) and through an REU supplement to that grant.

References and Notes

- (1) Yamakawa, H. *Modern Theory of Polymer Solutions*; Harper & Row: New York, 1971.
- (2) Oono, Y. *Adv. Chem. Phys.* **1985**, *61*, 301.
- (3) Freed, K. *Renormalization Group Theory of Macromolecules*; Wiley: New York, 1987.
- (4) des Cloizeaux, J.; Jannink, G. *Polymers in Solution: Their Modelling and Structure*; Clarendon Press: Oxford, England, 1990.
- (5) Cassassa, E. F., and Berry, G. C. In *Comprehensive Polymer Science*; Allen, G., Bevington, J. C., Eds.; Pergamon Press: Oxford, England, 1989; Vol. 2, Chapter 3.
- (6) Fujita, H. *Polymer Solutions*; Elsevier: Amsterdam, 1990.
- (7) Yamakawa, H. *Helical Wormlike Chains in Polymer Solutions*; Springer-Verlag: New York, 1997.
- (8) Fujita, H. *Macromolecules* **1988**, *21*, 179.
- (9) Graessley, W. W.; Hayward, R. C.; Grest, G. S. *Macromolecules* **1999**, xxxx.
- (10) Davidson, N. S.; Fetters, L. J.; Funk, W. G.; Hadjichristidis, N.; Graessley, W. W. *Macromolecules* **1987**, *20*, 2614.
- (11) Berry, G. C. *J. Chem. Phys.* **1966**, *44*, 4550; **1967**, *46*, 1338.
- (12) Abe, F.; Einaga, Y.; Yoshizaki, T.; Yamakawa, H. *Macromolecules* **1993**, *26*, 1884.
- (13) Einaga, Y.; Miyaki, Y.; Fujita, H. *J. Polym. Sci., Polym. Phys. Ed.* **1979**, *17*, 2103.
- (14) Abe, F.; Einaga, Y.; Yamakawa, H. *Macromolecules* **1993**, *26*, 1891.
- (15) Einaga, Y.; Koyama, H.; Konishi, T.; Yamakawa, H. *Macromolecules* **1989**, *22*, 3419.
- (16) Arai, T.; Abe, F.; Yoshizaki, T.; Einaga, Y.; Yamakawa, H. *Macromolecules* **1995**, *28*, 3609.
- (17) Yamada, T.; Yoshizaki, T.; Yamakawa, H. *Macromolecules* **1992**, *25*, 377.
- (18) Yamakawa, H.; Abe, F.; Einaga, Y. *Macromolecules* **1993**, *26*, 1898.
- (19) Konishi, T.; Yoshizaki, T.; Yamakawa, H. *Macromolecules* **1991**, *24*, 5614.
- (20) Yamamoto, Y.; Fujii, M.; Tanaka, G.; Yamakawa, H. *Polym. J.* **1971**, *2*, 799.
- (21) Fukuda, M.; Fukutomi, M.; Kato, Y.; Hashimoto, T. *J. Polym. Sci., Polym. Phys. Ed.* **1974**, *12*, 871.
- (22) Altares, T., Jr.; Wyman, D. P.; Allen, V. R. *J. Polym. Sci. A* **1964**, *2*, 4533.
- (23) Fetters, L.; Hadjichristidis, N.; Lindner, J. S.; Mays, J. W. *J. Phys. Chem. Ref. Data* **1994**, *23*, 619.
- (24) Tamai, Y.; Konishi, T.; Einaga, Y.; Fujii, M.; Yamakawa, H. *Macromolecules* **1990**, *23*, 4067.
- (25) Abe, F.; Horita, K.; Einaga, Y.; Yamakawa, H. *Macromolecules* **1994**, *27*, 725.
- (26) Kamijo, M.; Sawatari, N.; Konishi, T.; Yoshizaki, T.; Yamakawa, H. *Macromolecules* **1994**, *27*, 5697.
- (27) Fuji, Y.; Tamai, Y.; Konishi, T.; Yamakawa, H. *Macromolecules* **1991**, *24*, 1608.
- (28) Kamijo, M.; Abe, F.; Einaga, Y.; Yamakawa, H. *Macromolecules* **1995**, *28*, 1095.
- (29) Arai, T.; Sawatari, N.; Yoshizaki, T.; Einaga, Y.; Yamakawa, H. *Macromolecules* **1996**, *29*, 2309.
- (30) Sawatari, N.; Konishi, T.; Yoshizaki, T.; Yamakawa, H. *Macromolecules* **1995**, *28*, 1089.
- (31) Abe, F.; Einaga, Y.; Yamakawa, H. *Macromolecules* **1994**, *27*, 3262.
- (32) Kamijo, M.; Abe, F.; Einaga, Y.; Yamakawa, H. *Macromolecules* **1995**, *28*, 4159.
- (33) Matsumoto, T.; Nishioka, N.; Fujita, H. *J. Polym. Sci. A-2* **1972**, *10*, 23.
- (34) Osa, M.; Abe, F.; Yoshizaki, T.; Einaga, Y.; Yamakawa, H. *Macromolecules* **1996**, *29*, 2302.
- (35) Abe, F.; Einaga, Y.; Yamakawa, H. *Macromolecules* **1991**, *24*, 4423.
- (36) Fetters, L. J.; Hadjichristidis, N.; Lindner, J. S.; Mays, J. W.; Wilson, W. W. *Macromolecules* **1991**, *24*, 3127.
- (37) Chance, R. R.; Baniukiewicz, S. P.; Mintz, D.; Ver Strate, G.; Hadjichristidis, N. *Int. J. Polym. Anal. Charact.* **1995**, *1*, 3.
- (38) Yamada, M.; Osa, M.; Yoshizaki, T.; Yamakawa, H. *Macromolecules* **1997**, *30*, 7166.
- (39) Yamada, T.; Koyama, H.; Yoshizaki, T.; Einaga, Y.; Yamakawa, H. *Macromolecules* **1993**, *26*, 2566.
- (40) Horita, K.; Sawatari, N.; Yoshizaki, T.; Einaga, Y.; Yamakawa, H. *Macromolecules* **1995**, *28*, 4455.
- (41) Zilliox, J. G.; Roovers, J. E. L.; Bywater, S. *Macromolecules* **1975**, *8*, 573.
- (42) Colby, R. H.; Fetters, L. J.; Graessley, W. W. *Macromolecules* **1987**, *20*, 2226.
- (43) Hadjichristidis, N.; Zhongde, X.; Fetters, L.; Roovers, J. J. *J. Polym. Sci., Polym. Phys. Ed.* **1982**, *20*, 743.
- (44) Matsumoto, T.; Nishioka, N.; Fujita, H. *J. Polym. Sci., Polym. Phys. Ed.* **1972**, *10*, 23.
- (45) Tsuji, T.; Fujita, H. *Polym. J.* **1973**, *4*, 409.
- (46) Varma, B. K.; Fujita, H.; Takahashi, M.; Nose, T. *J. Polym. Sci., Polym. Phys. Ed.* **1984**, *22*, 1781.
- (47) Miyaki, Y.; Einaga, Y.; Fujita, H. *Macromolecules* **1978**, *11*, 1180.
- (48) Einaga, Y.; Miyaki, Y.; Fujita, H. *J. Polym. Sci., Polym. Phys. Ed.* **1979**, *17*, 2103.
- (49) Miyaki, Y.; Einaga, Y.; Fujita, H.; Fukada, M. *Macromolecules* **1980**, *13*, 588.
- (50) Huber, K.; Bantle, S.; Lutz, P.; Burchard, W. *Macromolecules* **1985**, *18*, 1461.
- (51) Bantle, S.; Schmidt, M.; Burchard, W. *Macromolecules* **1991**, *24*, 5729.
- (52) Sokal, A. D. In *Monte Carlo and Molecular Dynamics Simulations in Polymer Science*; Binder, K., Ed.; Oxford University Press: Oxford, England, 1995; pp 47–124.
- (53) LeGuillou, J. L.; Zinn-Justin, J. *J. Phys.* **1989**, *50*, 1365 and references therein to earlier work.
- (54) Domb, C.; Barnett, A. J. *Polymer* **1976**, *17*, 179. Our eq 16 is eq 20 of this paper.
- (55) Zoller, P.; Walsh, D. *Standard Pressure–Volume–Temperature Data for Polymers*; Technomic: Lancaster, PA, 1995.
- (56) The packing fraction for polymeric liquids is estimated from the random close-packed value for hard sphere liquids,⁵⁷ $\phi_{rcp} = 0.66$, and the reduced volume for typical polymeric liquids,⁵⁸ $v/v_0 = 1.2$. Thus, $\phi = \phi_{rcp}/1.2 = 0.55$.
- (57) Woodcock, L. V.; Angell, C. A. *Phys. Rev. Lett.* **1981**, *47*, 1129.
- (58) Table VIII-2 In Prausnitz, J. M.; Lichtenthaler, R. N.; Gomes de Azevedo, E. *Molecular Thermodynamics of Fluid-Phase Equilibria*, 2nd ed.; **1986**, Prentice Hall: Englewood Cliffs, NJ, 1986.
- (59) Roovers, J. Private communication.
- (60) Berry, G. C. Private communication.